Study of Redundantly Actuated DELTA-Type Parallel Kinematic Mechanisms

B. Corves*, S. A. Shahidi**, M. Lorenz**, S. Charaf Eddine** and M. Hüsing***

**Burkhard Corves is the Director, **S. Amirreza Shahidi, Michael Lorenz and Sami Charaf Eddine are research assistants and ***Mathias Hüsing is the Deputy Director of the Department of Mechanism Theory and Dynamics of Machines, RWTH Aachen University, D-52072 Aachen, Germany (e-mail: {corves, shahidi, lorenz, charaf_eddine, huesing}@igm.rwth-aachen.de).*

Abstract. Due to their high precision and dynamic properties, parallel kinematic manipulators (PKM) are particularly suited for high-speed and high-accuracy object handling. In order to improve their stiffness, their payload capacity and their accuracy PKM can be optimized by using a redundant actuator configuration. Accordingly, additional actuators are added to PKM in order to generate an optimized performance. The objectives, in this context, are highly task dependent and can involve a wide range of the robot's topological and morphological parameters. Based on different tasks and optimization targets, robots with unique specifications can be designed. In this study redundancy is used to show the effect of topological parameters of redundantly actuated DELTA-type manipulators on general performance characteristics, such as the energy consumption of the robot. The topological characteristics of n-$\underline{\text{R}}$RPaR manipulators in combination with actuator capabilities are considered as variables. It is shown that by choosing a proper topology, it is possible to achieve a higher performance by an intelligent usage of different torque distributions that may result in a more efficient energy consumption.

Key words: Actuation Redundancy, PKM, n-$\underline{\text{R}}$RPaR, DELTA-type Robot, Force Capability

1 Introduction

The quality and performance of industrial robots and manipulators commonly is measured by their maximum payload, maximum handling velocity or by their precision given in a certain workspace. In terms of accuracy of fast object handling, parallel kinematic manipulators (PKM) are preferred to their serial counterparts due to their excellent precision, dynamics characteristics and stiffness regardless of their relatively small workspace [1]. Generally, these manipulators are equipped with a task-depended number of actuators represented by the required degree of freedom (DoF) [2]. In contrast, redundantly actuated parallel kinematic manipulators (RA-PKM) use more actuators than needed (over-actuated) in trade-off for a higher stiffness resulting in a higher precision and a more efficient torque distribution.

Over actuation of parallel kinematic manipulators can be achieved by means of *branch* and *in-branch* actuation redundancy ([3], [4]). In the context of the current study, an n-$\underline{\text{R}}$RPaR ($n \geq 3$) structure is analyzed, which is also known as a DELTA-

type branch-redundant PKM. Manipulators of the n-$\underline{\text{R}}$RPaR-type are able to execute motion tasks in three translational degrees of freedom (DoF) as a result of their specific structure including parallelogram members [5].

Characterizing the manipulator based on time is of importance to optimize their performance in many aspects as object handling and assembly [6], which are discussed for the presented manipulator in Sections 2 and 3.

The objective to be pursued in current study is the effect of redundancy on general performance characteristics, such as the force capability of n-$\underline{\text{R}}$RPaRs. Two topologies with one and three degrees of redundancy are introduced [4], of which the one with four arms is supposed to be reconfigurable. There are different methods to study the force capability of (redundant)-PKM in which the screw theory is widespread used [7], [8], [9]. The procedure used in this contribution is mainly based on the one introduced by [4].

2 Inverse Kinematics

Determining the joint space parameters of the n-$\underline{\text{R}}$RPaR by given operational space parameters is discussed in this section. The special case of $n = 3$ with uniformly distributed arms characterises the conventional DELTA robot. The joint space parameters q of the manipulator can be extracted in the same way as DELTA robot. The kinematic parameters of the active and passive joints are as (see Figure 1):

$$\phi_{3,i} = \cos^{-1}\left(\frac{{}^{i}r_{i,y}}{l_{2,i}}\right) \tag{1a}$$

$$\phi_{2,i} = \cos^{-1}\left(\frac{{}^{i}r_{i,x}^2 + {}^{i}r_{i,y}^2 + {}^{i}r_{i,z}^2 - l_{1,i}^2 - l_{2,i}^2}{2\,l_{1,i}\,l_{2,i}\,\sin(\phi_{3,i})}\right) \tag{1b}$$

$$q_i = \tan^{-1}\left(\frac{-\kappa\,{}^{i}r_{i,x} + \zeta\,{}^{i}r_{i,z}}{\zeta\,{}^{i}r_{i,x} + \kappa\,{}^{i}r_{i,z}}\right) \text{ with: } \begin{cases} \zeta = l_{2,i}\sin(\phi_{3,i})\cos(\phi_{2,i}) + l_{1,i} \\ \kappa = l_{2,i}\sin(\phi_{3,i})\sin(\phi_{2,i}) \end{cases} \tag{1c}$$

The time differentiation of the closed form equation of the end-effector position can be exploited in order to determine the angular velocity of the crank and forearms of each linkage:

$$\mathbf{P}_{ee} = \mathbf{l}_{1,i} + \mathbf{l}_{2,i} + \mathbf{a} - \mathbf{b} \quad \therefore \quad \dot{\mathbf{P}}_{ee} = \dot{\mathbf{q}}_i \times \mathbf{l}_{1,i} + \omega_{2,i} \times \mathbf{l}_{2,i}, \tag{2}$$

where $\dot{\mathbf{q}}_i$ and $\omega_{2,i}$ are the rotational velocities of the crank and forearm of branch i respectively. The vector $\omega_{2,i} \times \mathbf{l}_{2,i}$ turns to zero by post dot multiplying both sides of (2) by $\mathbf{l}_{2,i}$ due to perpendicularity. Using the equation for angular velocity of the active joint ($\mathbf{R}_i$ is the rotation matrix of branch i of the manipulator to the global coordinate system and $\mathbf{R}_{i|2}$ represents the second column of matrix $\mathbf{R}_i$):

$$\dot{\mathbf{q}}_i = \mathbf{R}_i\,\dot{q}_i\,[0\,,1\,,0]^T = \dot{q}_i\,\mathbf{R}_{i|2}, \tag{3}$$

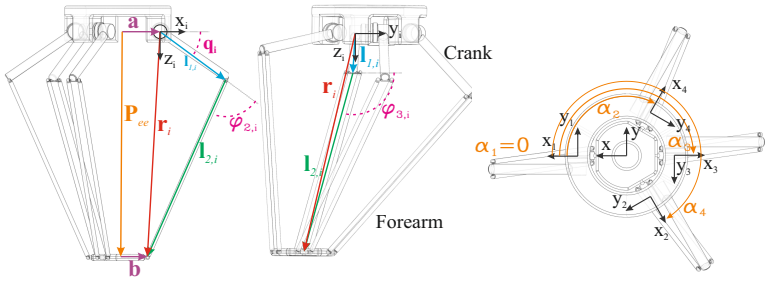

Fig. 1 Please write your figure caption here

and replacing the cross multiplication by the asymmetric matrix product (represented by $[\bullet]^c$), (2) can be rewritten in algebraic form:

$$\mathbf{l}_{2,i}^T \cdot \dot{\mathbf{P}}_{ee} = \mathbf{l}_{2,i}^T \left(\dot{q}_i [\mathbf{R}_{i|2}]^c \, \mathbf{l}_{1,i} \right). \tag{4}$$

Stacking (4) for different linkages results in (the dimensions are inserted for clarity):

$$\left[\left[\mathbf{l}_{2,r}^T \right]_{(1,3)} \otimes \mathbf{1}_{(n,1)} \right]_{(n,3)} \cdot \dot{\mathbf{P}}_{ee(3,1)} = \left[\dot{q}_r \otimes \mathbf{I}_n \right]_{(n,n)} \cdot \left[\left[\mathbf{l}_{2,r}^T \right]_{(1,3)}, \otimes \mathbf{I}_n \right]_{(n,3n)} \cdot \left[[\mathbf{R}_{i|2}]^c \otimes \mathbf{I}_n \right]_{(3n,3n)} \cdot \left[\left[\mathbf{l}_{1,r} \right]_{(1,3)} \otimes \mathbf{1}_{(n,1)} \right]_{(3n,1)}, \tag{5}$$

where the operator $\otimes$ represents the Kronecker product and the subscript r determines the *row*-index of the succeeding matrix. In order to simplify (5), the auxiliary matrix $[\mathbf{J}_{aux}]$ can be introduced as:

$$\left[\left[\mathbf{l}_{2,r}^T \right]_{(1,3)} \otimes \mathbf{1}_{(n,1)} \right]_{(n,3)} \cdot \dot{\mathbf{P}}_{ee(3,1)} = \left[\dot{q}_r \otimes \mathbf{I}_n \right]_{(n,n)} \cdot \left[\mathbf{J}_{aux} \right]_{(n,1)}. \tag{6}$$

Since the relation between workspace and joint space velocities is of interest, the right hand side of (6) can be rearranged according to:

$$\left[\left[\mathbf{l}_{2,r}^T \right]_{(1,3)} \otimes \mathbf{1}_{(n,1)} \right]_{(n,3)} \cdot \dot{\mathbf{P}}_{ee(3,1)} = \left[\mathbf{J}_{aux}(r,1) \otimes \mathbf{I}_n \right]_{(n,n)} \cdot \left[\dot{q}_r \otimes \mathbf{1}_{(n,1)} \right]_{(n,1)}. \tag{7}$$

The matrix $\left[\mathbf{J}_{aux}(r,1) \otimes \mathbf{I}_n \right]_{(n,n)}$ in (7) is a full rank diagonal matrix. Therefore, pre-multiplying both sides of (7) by $\left[\mathbf{J}_{aux}(r,1) \otimes \mathbf{I}_n \right]_{(n,n)}^{-1}$ results in the Jacobian matrix:

$$\left[\dot{q}_r \otimes \mathbf{1}_{(n,1)} \right]_{(n,1)} = \left[\mathbf{J}_{aux}(r,1) \otimes \mathbf{I}_n \right]_{(n,n)}^{-1} \left[\left[\mathbf{I}_{(2,r)}^T \right] \otimes \mathbf{1}_{(n,1)} \right]_{(n,3)} \cdot \dot{\mathbf{P}}_{ee(3,1)}, \tag{8}$$

or in short form:

$$\left[\dot{Q} \right]_{(n,1)} = \left[\mathbf{J}_v \right]_{(n,3)} \cdot \dot{\mathbf{P}}_{ee(3,1)}. \tag{9}$$

3 Inverse Dynamics

Considering the n-RRPaR as a time-invariant holonomic mechanical system, the principle of virtual works can be used to generalize the inverse dynamic. Acceleration of active and passive joints can be derived by second time derivation of (2):

$$\ddot{\mathbf{P}}_{ee} = \ddot{\mathbf{q}}_{1,i} \times \mathbf{l}_{1,i} + \dot{\mathbf{q}}_i \times (\dot{\mathbf{q}}_i \times \mathbf{l}_{1,i}) + \dot{\omega}_{2,i} \times \mathbf{l}_{2,i} + \omega_{2,i} \times (\omega_{2,i} \times \mathbf{l}_{2,i}). \quad (10)$$

Post dot-multiplying (10) by $\mathbf{l}_{2,i}$ and performing algebraic simplifications, the joint space acceleration given work space acceleration can be presented:

$$\ddot{q}_i = \frac{\mathbf{l}_{2,i}^T \left(\ddot{\mathbf{P}}_{ee} + (\dot{\mathbf{q}}_i \cdot \dot{\mathbf{q}}_i)\, \mathbf{l}_{1,i} + (\dot{\mathbf{q}}_i \cdot \dot{\mathbf{q}}_i)\, \mathbf{l}_{2,i}\right)}{\mathbf{l}_{2,i}^T \left[\mathbf{R}_{i|2}\right]^c \mathbf{l}_{1,i}} \quad \therefore \quad \ddot{\mathbf{q}}_{1,i} = \ddot{q}_i \mathbf{R}_{i|2}. \quad (11)$$

The angular acceleration of the forearm can be obtained, rearranging (10).

After defining the velocity and acceleration vectors, the force and moments associated to the end-effector and linkages can basically be driven in the same manner as the one for conventional topology of DELTA structures (for details see [10]):

$$\begin{aligned} 0 = {} & \delta[Q]_{(1,n)}^T\, [\tau]_{(n,1)} + \delta[\mathbf{X}_{ee}]_{(1,3)}^T \left[m_{ee}\left(\mathbf{g} - \ddot{\mathbf{P}}_{ee}\right)\right]_{(3,1)} + \\ & \sum_{i=1}^{n} \left(\delta^i[\mathbf{X}_{l_{1,i}}]_{(1,6)}^T \begin{bmatrix} m_{l_{1,i}} \left({}^i\mathbf{g} - {}^i\mathbf{a}_{1,i,c}\right) \\ {}^i\mathbf{I}_{1,i}\, {}^i\dot{\omega}_{1,i} + {}^i\dot{\mathbf{q}}_i \times \left({}^i\mathbf{I}_{1,i}\, {}^i\dot{\mathbf{q}}_i\right) \end{bmatrix}_{(6,1)} \right. \\ & \left. + 2\, \delta^i[\mathbf{X}_{l_{2,i}}]_{(1,6)}^T \begin{bmatrix} m_{l_{2,i}} \left({}^i\mathbf{g} - {}^i\mathbf{a}_{2,i,c}\right) \\ {}^i\mathbf{I}_{2,i}\, {}^i\dot{\omega}_{2,i} + {}^i\omega_{2,i} \times \left({}^i\mathbf{I}_{2,i}\, {}^i\omega_{2,i}\right) \end{bmatrix}_{(6,1)} \right). \end{aligned} \quad (12)$$

In (12) τ is the vector of manipulator torques, $\mathbf{g}$ represents the gravity, $\mathbf{I}$ is the inertia matrix, $\mathbf{a}$ stands for accelerations and subscript c refers to the center of mass. $\delta[\mathbf{X}_{ee}]$, $\delta^i[\mathbf{X}_{l_{1,i}}]$ and $\delta^i[\mathbf{X}_{l_{2,i}}]$ refer to infinitesimal deviations of the end-effector and the center of mass of the cranks and forearms respectively. $\delta[\mathbf{X}_{ee}]$ can be defined by means of the system Jacobian matrix as shown in (9). The link Jacobians $\mathbf{J}_{v1}^*$ and $\mathbf{J}_{v2}^*$, which relate the velocities of each link's center of mass to the work space velocity vector, are deployed for simplification:

$$\left\{\delta[Q],\, \delta^i[\mathbf{X}_{l_{1,i}}],\, \delta^i[\mathbf{X}_{l_{2,i}}]\right\} = \left\{[\mathbf{J}_v],\, [\mathbf{J}_{v1}^*],\, [\mathbf{J}_{v2}^*]\right\} \delta\left[\mathbf{X}_{ee}\right]. \quad (13)$$

Shortening the summation ($\sum$) part of (12) as link dynamics (*LD*) results in:

$$0 = \delta\left[\mathbf{X}_{ee}\right]_{(1,3)}^T [\mathbf{J}_v]_{(3,n)}^T\, [\tau]_{(n,1)} + \delta[\mathbf{X}_{ee}]_{(1,3)}^T \left[m_{ee}\left(\mathbf{g} - \ddot{\mathbf{P}}_{ee}\right)\right]_{(3,1)} + \delta\left[\mathbf{X}_{ee}\right]_{(1,3)}^T LD. \quad (14)$$

Thus, the dynamic burden of actuators can concisely be formulated as:

$$[\tau]_{(n,1)} = -\,[\mathbf{J}_v]_{(3,n)}^{+T} \left(\left[m_{ee}\left(\mathbf{g} - \ddot{\mathbf{P}}_{ee}\right)\right]_{(3,1)} + LD \right), \quad (15)$$

where $[\,]^+$ symbolizes the pseudo inverse.

4 Force capability

The topological structure of the n-RRPaR can be optimized with regard to different tasks considering an appropriate objective function. One of the possible objectives can be considered as the reachable force of the manipulator. In this section, the overall procedure in order to compute the force capability of the manipulator, with a concise formulation for the general structure, is sketched and discussed .

The classical relation between torque and force can be written for the cranks:

$$^i\mathbf{M}_i = {}^i\mathbf{l}_{1,i} \times {}^i\mathbf{F}_i. \quad \therefore \quad {}^i\mathbf{F}_i = -\frac{1}{l_{1,i}^2}\,{}^i\mathbf{l}_{1,i} \times {}^i\mathbf{M}_i. \tag{16}$$

In (16), ${}^i\mathbf{F}_i$ represents the resultant force of the actuator in the local coordinate system and:

$$^i\mathbf{l}_{1,i} = l_{1,i}\left[c\,(q_i),\ 0,\ s\,(q_i)\right]^T, \qquad {}^i\mathbf{M}_i = T_i\left[0,\ 1,\ 0\right]^T, \tag{17}$$

with T_i being the applicable torque of the i^{th} actuator. To transfer the equation to algebraic form, cross multiplications are replaced with the asymmetric matrix product. Simultaneously, the forces are transferred to the global coordinate system:

$$\mathbf{F}_i = -\frac{1}{l_{1,i}^2}\mathbf{R}_i\left[{}^i\mathbf{l}_{1,i}\right]^c\,{}^i\mathbf{M}_i = \mathbf{J}_{F,i}\,{}^i\mathbf{M}_i, \tag{18}$$

where $\mathbf{J}_{F,i}$ refers to the force Jacobian.

Considering the rods of the forearm as rigid bodies, which prevents the energy loss, the contribution of each actuator to the end-effector's force capability is equal to $\mathbf{F}_i$. Thus, the force capability of the manipulator on the end-effector results from summing up the individual forces:

$$\mathbf{F}_{(3,1)} = \Big[\mathbf{I}_3 \otimes \mathbf{1}_{1,n}\Big]_{(3,3n)} \cdot \Big[\mathbf{J}_{F,r} \otimes \mathbf{I}_n\Big]_{(3n,3n)} \cdot \Big[\mathit{Conversion\ Matrix}\Big]_{(3n,n)} \cdot \Big[\tau\Big]_{(n,1)}, \tag{19}$$

where index r in $J_{F,r}$ refers to the row index of the succeeding matrix and $[\mathit{Conversion\ Matrix}]$ is a sparse matrix containing ones at the indices $(3(i-1)+2\,,\,i)$ with $i = 1,\ldots,n$.

The method of scaling factors can be used to compute the maximum force capability of the manipulator [8], [7], [4]. In this method, the required torque to impose a force in a predefined direction of interest is computed by means of (19). The computed torques can be scaled by the factors resulting from the ratio of maximum applicable torques to the required amount and lastly the force is to be recalculated

by (19). In the present study, the Jacobian's null-space resolution is also used to optimize the maximum force as the one introduced in [9].

5 Results

To examine the presented idea two types of structure topologies are introduced in this section. The first structure is a 4-armed manipulator with varying torque capacity of actuators and adjustable configuration. The second structure is a 6-armed manipulator and considered to have a variable torque capacity of actuators. Different topologies and actuator capacities are listed in Table 1. The 4-armed manipulators in the three scenarios $4n-1$ to $4n-3$ have evenly distributed branches (i.e. α in Figure 1) and are supposed to have actuators with different torque capacities (the nominal torque of actuators are supposed to be 100 *Nm*). The remaining scenarios involve manipulators with varying topological configurations, with all actuators working with 100% capacity. The topology of the 6-armed manipulator is supposed to be unique (with evenly distributed arms) with varying capacities of actuators. For clarity, the topology for cases $4n-3$ to $4n-6$ are shown in Figure 2.

Table 1 Percentage of applicable torque of actuators in different simulation configurations

α	0	$\frac{\pi}{8}$	$\frac{\pi}{4}$	$\frac{\pi}{3}$	$\frac{3\pi}{8}$	$\frac{\pi}{2}$	$\frac{5\pi}{8}$	$\frac{2\pi}{3}$	$\frac{3\pi}{4}$	$\frac{7\pi}{8}$	π	$\frac{9\pi}{8}$	$\frac{5\pi}{4}$	$\frac{4\pi}{3}$	$\frac{11\pi}{8}$	$\frac{3\pi}{2}$	$\frac{13\pi}{8}$	$\frac{5\pi}{3}$	$\frac{7\pi}{4}$	$\frac{15\pi}{8}$
$4n-1$	100					10					100					10				
$4n-2$	50					50					50					50				
$4n-3$	100					100					100					100				
$4n-4$		100								100		100								100
$4n-5$			100						100				100						100	
$4n-6$					100		100								100		100			
$6n-1$	100			10				100			10			100				10		
$6n-2$	50			50				50			50			50				50		
$6n-3$	100			50				100			50			100				50		
$6n-4$	100			100				100			100			100				100		

Figure 2 shows the force distribution of a 4-armed manipulator, in which all the actuators are working with full power, in a plane in the middle of the workspace ($z=-0.775$ *m*). Two main topologies are selected, which are oriented complimentary to each other (i.e. $4n-3$ with $4n-5$ and $4n-4$ with $4n-6$). A preliminary examination exhibits choosing an appropriate orientation of the manipulator in a specific application can enhance the force capability of the manipulator in a direction of desire considerably. For instance, although the manipulators of cases $4n-3$ and $4n-5$ have a similar topology and the actuator capacities are the same, with a same z-force capability, there is almost 42% improvement in x and y-force capabilities for $4n-5$. The fact also holds for the manipulator with non-homogeneously distributed arms.

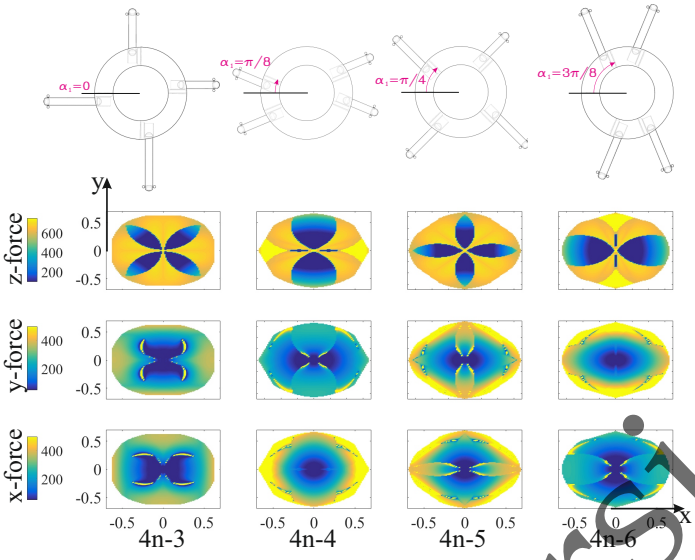

Fig. 2 4-armed manipulators with configurations $4n-3$ to $4n-6$

The force capabilities for the 4-armed manipulators are also computed all over the workspaces. The force expectations in different directions are shown in Figure 3. A comparison between $4n-1$ and $4n-2$ emphasizes on the importance of a well torque distribution and proves the advantages of task-oriented manipulators design.

The statistical study of the cases with 6 arms are also presented in Figure 3. The results are obtained from the examination of force capabilities in the effective workspace of the manipulator. Cases $6n-1$ and $6n-2$ show comparable force capabilities with a smoothly distributed torque capacity in case $6n-2$. Doubling the actuation of three actuators in $6n-2$ results in almost 50% higher force capability in case $6n-3$, but further doubling the actuation of remaining actuators would result in almost 32% more improvement (the force capability of $6n-4$ is twice as $6n-2$).

6 Conclusions

This study intends to examine the effect of actuation redundancy and topological configuration of a DELTA-type parallel manipulator on its kineto-statics performance. It is shown that a task oriented topological design of the robot can remarkably enhance its force capability. Furthermore, over-actuated manipulators proved to have a smooth torque distribution for specific performances, which may lead to more resource-efficient processes.

Further research in this field is accomplished by examining the manipulator flexibility by different topologies. Optimizations are to be performed to achieve a high

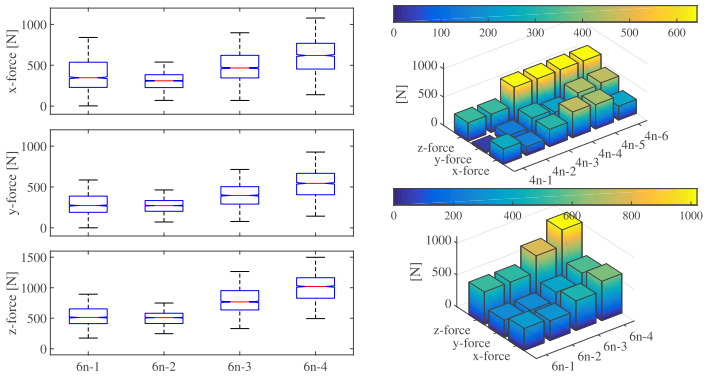

Fig. 3 Statistical examination of selected structures presented in Table 1

precision concerning the end-effector, adhering a high performance and energy-efficient task-oriented manipulation. The morphology of the robot can be determined, taking different objectives into consideration.

References

1. Merlet, J. P. (2012). Parallel robots (Vol. 74). Springer Science & Business Media.
2. Corves, B., Brinker, J., Lorenz, M., & Wahle, M. (2016). Design methodology for translational parallel manipulators exhibiting actuation redundancy. Proceedings of the Institution of Mechanical Engineers, Part C: Journal of Mechanical Engineering Science, 230(3), 425-436.
3. Pierrot F.,(2002). "Parallel mechanisms and redundancy." In 1st Int. Colloquium, Collaborative Research Centre 562, pages 261-277, Braunschweig, 29-30 Mai 2002
4. Lorenz, M., Corves, B., & Riedel, M. (2014, August). Kinetostatic performance analysis of a redundantly driven parallel kinematic manipulator. In ASME 2014 International Design Engineering Technical Conferences and Computers and Information in Engineering Conference (pp. V05BT08A080-V05BT08A080). American Society of Mechanical Engineers.
5. Clavel, R. (1990). U.S. Patent No. 4,976,582. Washington, DC: U.S. Patent and Trademark Office.
6. Biagiotti, L., & Melchiorri, C. (2008). Trajectory planning for automatic machines and robots. Springer Science & Business Media.
7. Garg, V., Nokleby, S. B., & Carretero, J. A. (2007, May). Force-Moment Capabilities of Redundantly-Actuated Spatial Parallel Manipulators Using Two Methods. In Proceedings of the 2007 CCToMM Symposium on Mechanisms, Machines, and Mechatronics, Montral, QC, Canada, May (p. 12).
8. Firmani, F., Zibil, A., Nokleby, S. B., & Podhorodeski, R. P. (2007). Force-moment capabilities of revolute-jointed planar parallel manipulators with additional actuated branches. Transactions of the Canadian Society for Mechanical Engineering, 31(4), 469-481.
9. Nokleby, S. B., Fisher, R., Podhorodeski, R. P., & Firmani, F. (2005). Force capabilities of redundantly-actuated parallel manipulators. Mechanism and machine theory, 40(5), 578-599.
10. Brinker, J., Corves, B., & Wahle, M. (2015, October). A comparative study of inverse dynamics based on clavels delta robot. In Proceedings of the 14th World Congress in Mechanism and Machine Science. Taipei, Taiwan (pp. 25-30).